IEICE TRANS. COMMUN., VOL. E75-B, NO. 1 JANUARY 1992

PAPER

A Fast Viterbi Decoding in Optical Channels

Hiroyuki YASHIMA†, Jouji SUZUKI†, Iwao SASASE††
and* Shinsaku MORI††, *Members

SUMMARY A fast Viterbi decoding technique with path reduction in optical channels is presented. This decoding exploits the asymmetric characteristic of optical channels. In the decoding trellis, the branches with low or no possibility being correct path are eliminated based on the detected signal level. The number of Add-Compare-Select (ACS) operations which occupy the dominant part of Viterbi decoding is considerably reduced due to branch eliminations, and fast decoding is realized by decoding asynchronously to received sequence. The reduction of the number of ACS operations is derived for the codes with rate 1/2. It is shown that the number of ACS operations is considerably reduced compared with the conventional Viterbi decoding. The bit error probability of the proposed decoding is derived for noiseless photon counting channel. It is also shown that the decoding technique can be applied to the cases using avalanche photo diode (APD) based receiver with dark current noise at a cost of negligible degradation on the bit error probability.

key words: *viterbi decoding, optical channel*

1. Introduction

Recently, there has been great interest in studying optical communication systems with fast data transmission. Since the performance degrades due to various factors, such as shot noise, dark current noise, energy loss and so on, coding technique is required to achieve higher reliability communications. It has been reported that Reed-Solomon codes or block codes are advantageous to obtain large degree of error correction capability for optical PPM signaling[1],[2].

On the other hand, it is well known that maximum likelihood sequence estimation, implemented with the Viterbi algorithm[3], with convolutional codes can provide significant improvement in performance due to its powerful error correction capability. It has been shown that convolutional codes and Viterbi decoding over optical OOK signaling yield significant coding gain[4]. However, in practical aspect, the complexity of Viterbi decoding makes it difficult to be applied in optical communication systems with high rate transmission. In Viterbi decoding, the path metrics of survival paths are calculated and new survival paths are selected by Add-Compare-Select (ACS) operations[5] on the merged states. The ACS operations occupy dominant part of decoding, and therefore, reduction of the number of ACS operations is useful to realize fast decoding in optical channels.

The characteristic of the optical channels is different from Gaussian one. The optical channel generally possesses asymmetrical characteristics, so that the error probability when laser is on is not always equal to that when laser is off. Especially in noiseless photon counting channel[6],[7], the error occurs only when the symbol 1 is transmitted, and the channel presents complete asymmetric characteristic called Z-channel. Therefore, there exist some paths with likelihood 0 when one or more photons are received.

In this paper, we propose a reduced-path Viterbi decoding (RPVD) in optical channels to achieve fast decoding of convolutional coded sequences by reducing the number of the ACS operations, based on the asymmetric characteristic of optical channels. In noiseless photon counting channel, there are some cases that the survival path can be determined without ACS operations because there are some paths with likelihood 0, which allows the maximum likelihood decoding with reducing the number of ACS operations. In the RPVD, the branches with low or no possibility being correct path are eliminated based on received signal level. Then, the number of merge events, in which the ACS operation should be done, in decoding trellis is considerably decreased. Therefore high speed decoding can be realized by decoding asynchronously to received sequence with buffers to save the sequence.

Section 2 presents the description of the RPVD. In Sect. 3, an analytical method to derive the reduction rate of the number of ACS operations is described. The performance of the RPVD on noiseless photon counting channel is obtained in Sect. 4. In Sect. 5, the RPVD is employed for a noisy channel. The performance of the RPVD is presented for the case in which the received signal is detected by an avalanche photo diode (APD) with dark current noise.

Manuscript received April 1, 1991.
Manuscript revised July 18, 1991.

† The authors are with the Faculty of Engineering, Saitama University, Urawa-shi, 338 Japan.
†† The authors are with the Faculty of Science and Technology, Keio University, Yokohama-shi, 223 Japan.

2. Reduced-Path Viterbi Decoding

The information sequence is coded by the convolutional code with rate 1/2, and transmitted over the optical channel as On-Off-Keying (OOK) signals. In the receiver, after detecting the signals, the sequence is decoded by the RPVD with the procedure described hereafter. Figure 1 shows an example of the probability density of the detector output in a case of an APD based receiver as a noisy channel, where p_0 is the density for transmitted symbol $y=0$, and p_1 for $y=1$. Thus, the optical channel generally possesses asymmetric characteristic, since the density of detected signal for $y=0$ is different from that for $y=1$. In the RPVD, a fast decoding is realized by exploiting the nature of the asymmetric characteristic of the optical channel.

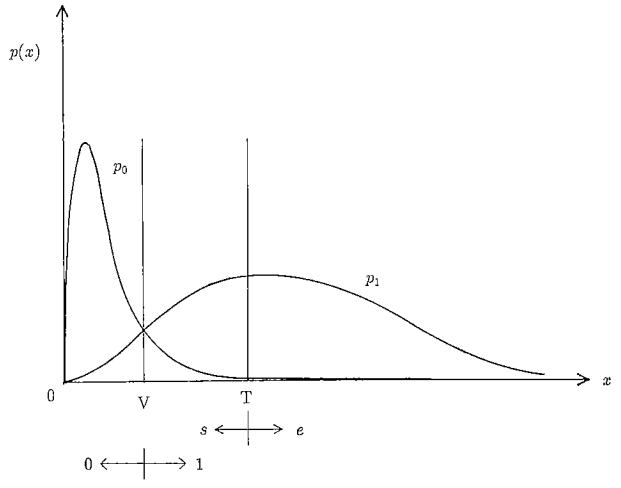

Fig. 1 Probability density of detected signals.

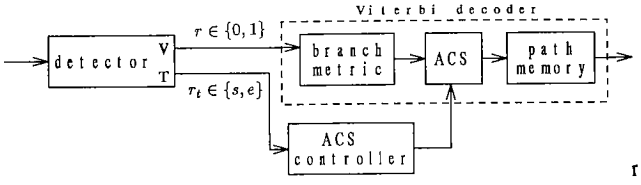

Fig. 2 Block diagram of RPVD.

Figure 2 shows the block diagram of the RPVD. In the conventional Viterbi decoding, the branch metric is calculated using detector output r decided by the threshold V, and the paths with larger likelihood are selected by ACS operations, and then, the maximum likelihood sequence is decoded. In the RPVD, the following procedure is added to the conventional Viterbi decoding. In the detector, the threshold T for branch elimination is set as in Fig. 1. The symbol r_t decided by T consist of $\{s, e\}$, where $r_t=e$ ("elimination" of branches) denotes the symbol larger than T and $r_t=s$ ("survival" of branches) denotes that smaller than T, and r_t is used only for branch elimination. The conditional probability $P_{(r_t|y)}$ is given, for $r_t=e$ and $y=0$, by

$$P_{(e|0)}=\int_T^\infty p_0(x)\,dx, \qquad (1)$$

and T is set so that $P_{(e|0)}$ is very small. This denotes that the transmitted symbol y must be 1 with very high possibility when $r_t=e$. Then, for $r_t=e$, y is regarded as 1 and the ACS controller eliminates the branches with corresponding symbol 0 from the candidates of maximum likelihood path, because the possibility of $y=0$ is very small. Thus, the branches with low possibility being correct path are eliminated and the number of merge events is considerably reduced. The ACS controller detects the merged states which need ACS operation, and the sequence is decoded with reduced number of ACS operations.

Here, we show a simple example of the case using the encoder with constraint length $k=3$ shown in Fig. 3(a). Figure 3(b) shows the corresponding four state trellis diagram. At the first level, the detector output r_t is *ss* and all branches survive. When $r_t=se$ as at the second level, the second symbol is regarded as 1 and the branches whose second symbol is 0 (00 and

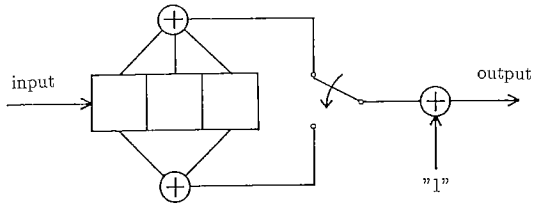

(a)

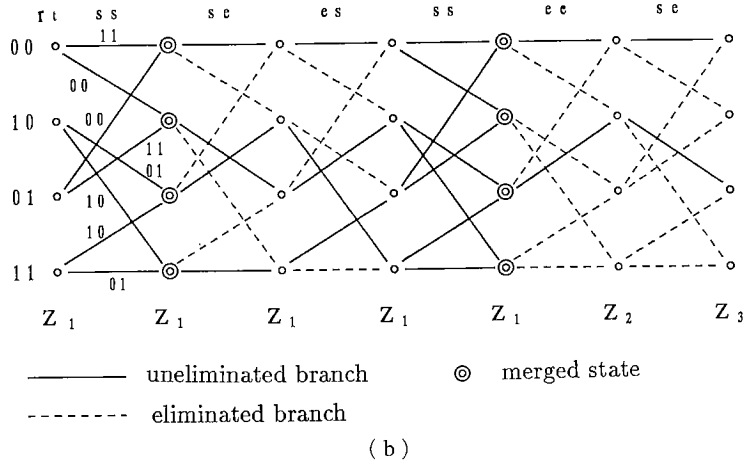

(b)

Fig. 3(a) Convolutional encoder with rate 1/2 and $k=3$.
(b) Trellis diagram of RPVD.

10) are eliminated. Note that the merge event does not occur on all states. Similarly, for $r_t = es$ as at the third level, the branches whose first symbol is 0 such as 00 or 01 are eliminated. Further, for $r_t = ee$ as at the fifth level, six branches including symbol 0 are eliminated and only two branches and two states can survive without merging. At the next step, branches are extended only from these survival states. Thus, the branches with low certainty to be correct path are eliminated according to the detected signal level r_t. Consequently, the RPVD reduces many paths from the candidates of the maximum likelihood path before ACS operations, and the number of merge events, namely, ACS operation is considerably reduced due to the path reduction.

While eliminating branches, the branch metrics are calculated using r and are saved in the buffers of the metric, and the symbols are asynchronously decoded to the received sequence. Then, fast decoding can be realized by reducing total number of ACS operations.

In the encoder in Fig. 3(a), we complement the output symbol due to following reason. If we use the encoder with noncomplement output, when more than three consecutive *ee* are received, all path are truncated in the trellis. To prevent this event, we complement the output symbol of the encoder. Hence, the path of (11, 11, 11,$\cdots$) always survives.

In the noiseless photon counting channel, $P_{(e|0)}$ is 0 as described in Sect. 4. Therefore, the correct path is never eliminated by branch elimination, which dose not affect the bit error probability performance.

Table 1 Transition of the survival state set and the number of ACS operations.

state	r_t	next state	number of ACS
Z_1	ss	Z_1	4
	se	Z_1	0
	es	Z_1	0
	ee	Z_2	0
Z_2	ss	Z_1	0
	se	Z_3	0
	es	Z_4	0
	ee	Z_5	0
Z_3	ss	Z_2	2
	se	Z_2	0
	es	Z_2	0
	ee	Z_2	0
Z_4	ss	Z_1	0
	se	Z_4	0
	es	Z_3	0
	ee	Z_5	0
Z_5	ss	Z_2	0
	se	Z_5	0
	es	Z_5	0
	ee	Z_5	0

3. Reduction of the Number of ACS Operations

We now derive the reduction ratio of the number of ACS operations, considering the case with the encoder and trellis diagram shown in Fig. 3(a) and 3 (b), respectively. Here, we define survival state set to show the combinations of survival states in decoding trellis. At a node level, five survival state sets can be considered as,

$$\begin{aligned} &Z_1\text{: } (00, 10, 01, 11)\\ &Z_2\text{: } (00, 10)\\ &Z_3\text{: } (00, 01)\\ &Z_4\text{: } (00, 11)\\ &Z_5\text{: } (00). \end{aligned} \tag{2}$$

For example, Z_1 denotes the event that all of four states survive and Z_2 denotes that the survival states are 00 and 10. There exist only those five kinds of survival state sets and it transits Z_1, Z_1, Z_1, Z_1, Z_1, Z_2, Z_3 in the case of Fig. 3(b). The transition of survival state sets at the next node level and the number of merged states in which ACS operation should be done are listed in Table 1. The number of ACS operations is four for the transition from Z_1 to Z_1 with $r_0 = ss$ and two for the transition from Z_3 to Z_2 with $r_0 = ss$. Figure 4 shows the state transition diagram of survival state sets. The transition probabilities are shown beside the corresponding transition path, where P_s and P_e are the event probabilities of $r_t = s$ and $r_t = e$, respectively. The transition probability matrix Π is given by

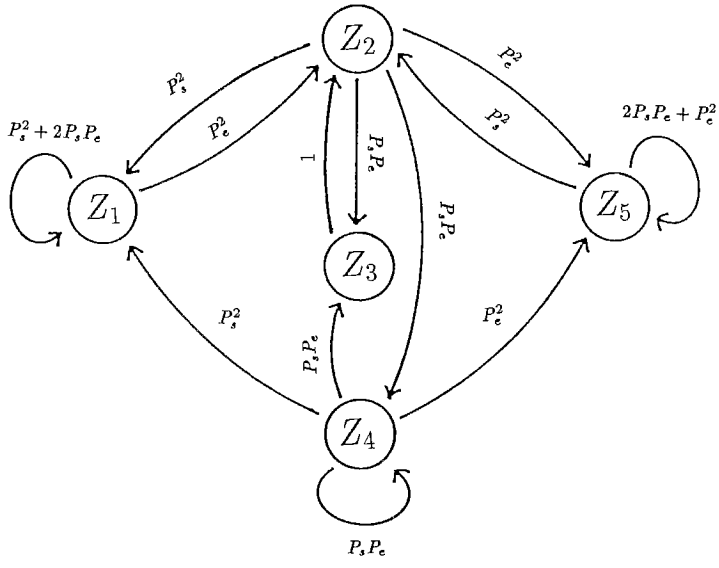

Fig. 4 State transition diagram of the survival state sets.

$$\Pi=\begin{bmatrix} P_s^2+2P_sP_e & P_e^2 & 0 & 0 & 0 \\ P_s^2 & 0 & P_sP_e & P_sP_e & P_e^2 \\ 0 & 1 & 0 & 0 & 0 \\ P_s^2 & 0 & P_sP_e & P_sP_e & P_e^2 \\ 0 & P_s^2 & 0 & 0 & 2P_sP_e+P_e^2 \end{bmatrix} \tag{3}$$

where ij-th element shows the transition probability from Z_i to Z_j. Since Π is regular Markov source, the stationary state distribution Z can be obtained by using the following conditions,

$$\begin{aligned} &Z\Pi=Z \\ &\sum_{i=1}^{5} Z_i=1 \\ &Z_i\geqq 0 \end{aligned} \tag{4}$$

as

$$Z=\left[\frac{P_s}{P_e^3}g\left(\frac{1}{P_sP_e}-1\right)g \quad g \quad g\frac{P_e}{P_s^3}g\right] \tag{5}$$

where

$$g=\frac{P_s^3P_e^3}{P_s^4+P_s^2P_e^2+P_s^3P_e^3+P_e^4}. \tag{6}$$

Then, the average number of ACS operations to decode a symbol is obtained by

$$n_{\mathrm{RPVD}}=4\frac{P_s^3}{P_e^3}g+2P_s^2g. \tag{7}$$

Whereas, the average number of ACS operations in the conventional Viterbi decoding is

$$n_{\mathrm{VD}}=4. \tag{8}$$

Figure 5 shows the relation between the ACS rate, denoted by $n_{\mathrm{RPVD}}/n_{\mathrm{VD}}$, and P_e. It is found that the number of ACS operations can be reduced up to 22% of that of conventional Viterbi decoding at $P_e=0.4$, and 9% at $P_e=0.5$ for $k=3$.

The presented method to derive the ACS rate can be generalized for the codes with larger k by extending the matrix Π, though the derivation of Π and Z is rather tedious because the matrix Π becomes huge for large k. The simulation results for $k=4$ and 5 are also shown in Fig. 5. Note that the ACS rate for $k=3$-5 possesses similar tendency. This is because the probability to eliminate a branch depends almost only on P_e and the survival ratio of branches at a node level is almost independent of constraint length k, as for the codes with same code rate.

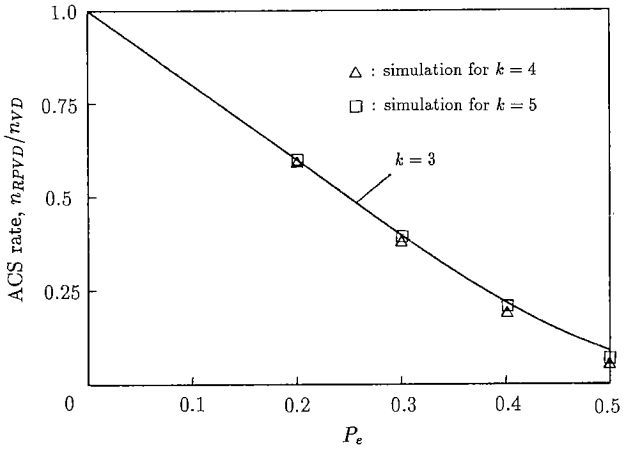

Fig. 5 Normalized number of ACS operations.

4. Performance of the RPVD in Noiseless Photon Counting Channel

In this section, the performances of the RPVD in noiseless photon counting channel[6]-[9] are presented.

For the noiseless channel, a light source as a laser transmits photons with an average of n photons when $y=1$ is transmitted, while no photon is transmitted for $y=0$. In the receiver, photons are detected by the photon counter. When $y=1$ is transmitted, the number of detected photon has a Poisson distribution

$$P_n(x)=\frac{n^xe^{-n}}{x!} \quad (x=0, 1, 2, \cdots). \tag{9}$$

where n is the mean number. We let the received symbol $r=1$ when one or more photons are received and $r=0$ when no photons are received. Then, the probability $P_{(r|y)}$ that no photon is detected for $y=1$ is given

$$\begin{aligned} P_{(0|1)}&=P_n(0) \\ &=e^{-n}. \end{aligned} \tag{10}$$

Whereas the probability of detecting no photons when $y=0$ is transmitted is equal to 1. The channel characteristic of noiseless photon counting channel is shown in Fig. 6. In the RPVD, when one or more photons are received, the branches corresponding symbol 0 are eliminated because of $P_{(1|0)}=0$. Then, we also define $r_t=s$ for the reception of no photons and $r_t=e$ for one

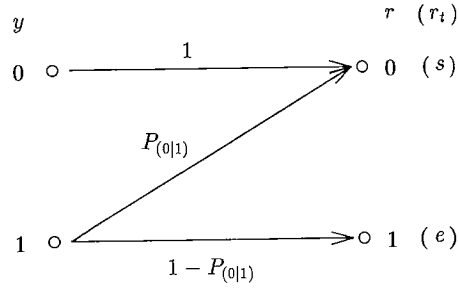

Fig. 6 Channel characteristic of noiseless photon counting channel.

or more photons.

Here, we derive the bit error probability of the RPVD in the noiseless channel. In the above mentioned condition, the correct paths are never eliminated by the branch elimination as shown by $P_{(e|0)}=0$. Then, the bit error probability of the RPVD is equal to that of Viterbi decoding. The bit error probability using rate 1/2 convolutional code in general memoryless channel is tightly upperbounded by[3],[4]

$$P_b < \sum_{J=d}^{\infty} C_J P_J \tag{11}$$

where d is free distance of the code, P_J is the first-event error probability to select an incorrect path of distance J, and C_J satisfies

$$\left.\frac{dT(D,F)}{dF}\right|_{F=1} = \sum_{J=d}^{\infty} C_J D^J \tag{12}$$

where $T(D, F)$ is the generating function of the code, D is branch gain and F is concerned with information bits. In this channel, P_b and P_J depend on the transmitted data sequences $\boldsymbol{a}_i$ due to asymmetric characteristic. Then, P_b is represented by averaging conditional probability for all sequences $\boldsymbol{a}$ as

$$P_b < \left[\sum_{J=d}^{\infty} C_J P_{J(a_i)}\right]_a = \sum_{J=d}^{\infty} C_J [P_{J(a_i)}]_a \tag{13}$$

where $P_{J(a_i)}$ is first-event error probability conditioned on a sequence $\boldsymbol{a}_i$, and $[\cdot]_a$ denotes average with respect to all sequences $\boldsymbol{a}$.

Let us consider the condition to select incorrect path. Assume the case in which a transmitted sequence includes four 1 and one 0 on the five different bit positions between correct and incorrect paths of distance 5. In this case, only when all of four 1 are erased (received as 0), incorrect path is selected. It is because if at least one 1 is received, the likelihood function on the incorrect path becomes 0 because of $P_{(1|0)}=0$, and then the correct path is selected. Thus, incorrect path is selected in the following case. There exist symbols 1 equal to or more than $d/2$ in the correct path on the different bit positions between correct and incorrect paths, and all of the transmitted symbols 1 are received as 0. Then, the first-event error probability conditioned on a sequence $\boldsymbol{a}_i$ is given by

$$P_{J(a_i)} = P_{(0|1)}^{l} \tag{14}$$

where l is the number of symbols 1 on the different bit positions in the sequence $\boldsymbol{a}_i$. As mentioned in Ref. (4), in the pairs of correct and incorrect paths with distance d, there are d different bit positions, and the positions are same regardless of encoder input sequences. In order to get the averaged first-event error probability $[P_{J(a_i)}]_a$, we need the distribution of l for all sequences $\boldsymbol{a}$ with same different bit positions. The distribution of l for all sequences $\boldsymbol{a}$ with same different bit positions can be given as the weight distribution $p_Q(l)$ derived in Ref. (4). Thus, the first-event error probability is given by

$$[P_{J(a_i)}]_a = \begin{cases} \displaystyle\sum_{l=(J+1)/2}^{J} p_{Q(l)} P_{(0|1)}^{l} \\ \quad : \text{for odd } J, \\ \displaystyle\frac{1}{2} p_{Q(J/2)} P_{(0|1)}^{J/2} + \sum_{l=J/2+1}^{J} p_{Q(l)} P_{(0|1)}^{l} \\ \quad : \text{for even } J. \end{cases} \tag{15}$$

Using Eqs. (13) and (15), the upper bound of bit error probability of the RPVD is given and the bound versus average transmitted photons $\langle k_1 \rangle$ for symbol 1 is shown in Fig. 7 together with simulated results for $k=3$. It can be seen that the simulation results well agree with the theoretical one.

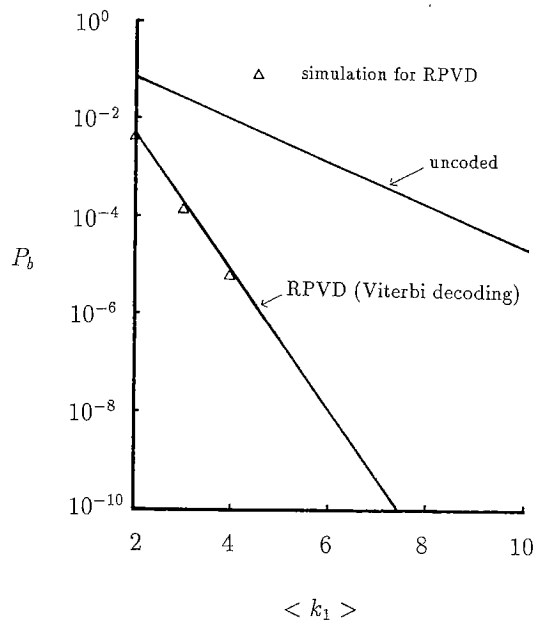

Fig. 7 Bit error probability on the noiseless photon counting channel for $k=3$.

In this channel, all branches with corresponding symbol 0 are eliminated for $r_t=e$ $(r=1)$. When the probabilities of information symbols 0 and 1 are equal, the transmitted symbols y consist of 0 and 1 with equal probabilities at the output of the encoder shown in Fig. 3(a). When the average number n of photons is enough, P_e is almost equal to 0.5 because of $P_{(s|1)} \approx 0$. Then, the ACS rate is reduced to

$$\frac{n_{\mathrm{RPVD}}}{n_{\mathrm{VD}}}(P_e \approx 0.5) \approx 0.09. \tag{16}$$

Thus, the number of ACS operations can be considerably reduced without degradation on the bit error probability in the noiseless photon counting channel.

5. Performance of the RPVD Using APD-Based Receivers

In this section, we present the performances of the RPVD with hard decision in the case using APD-based receivers with dark current noise[10),(11)] as an example of noisy channels.

The received signal is detected by APD. When 1 is transmitted, the light pulse injects k_1 electrons into the APD; these have Poisson distribution with mean value

$$E\langle k_1\rangle = N_s + N_d \tag{17}$$

where N_s is the mean number due to the pulse and N_d represents dark current. When 0 is transmitted, the number of electrons k_0 has also Poisson distribution with mean value

$$E\langle k_0\rangle = N_d. \tag{18}$$

The APD generates secondary output electrons x from Poisson distributed primaries. The probability density of the output is well approximated by Ref. (11)

$$P(x|n) = \left[\frac{1}{\left[1+\frac{x-nG}{\sigma\lambda}\right]^{3/2}}\right]\left[\frac{1}{[2\pi\sigma^2]^{1/2}}\right] \cdot \exp\left[-\frac{(x-nG)^2}{2\sigma^2\left(1+\frac{x-nG}{\sigma\lambda}\right)}\right] \tag{19}$$

$$\sigma^2 = nG^2F$$

$$\lambda = \frac{(nF)^{1/2}}{F} - 1$$

$$F = \varepsilon G + \left(2-\frac{1}{G}\right)(1-\varepsilon) \tag{20}$$

where ε is the APD ionization coefficient, G is the gain of the APD, and n is the average primary electrons. An example of the probability density of the APD output is shown in Fig. 1.

Here, let us assume that the threshold T is set so that $P_{(e|0)}$ is very small and the threshold V is determined by numerical integration so as to minimize the error probability P_E, when transmitted symbols 0 and 1 are equally frequent, where

$$P_E = \frac{1}{2}\left[\int_V^{\infty} p_0(x)\,dx + \int_{-\infty}^{V} p_1(x)\,dx\right]. \tag{21}$$

For this threshold V, the channel characteristic is well approximated to BSC. The bit error probability for hard decision Viterbi decoding is obtained by Ref. (3). In the RPVD, while eliminating branches using r_t decided by T, the metrics are calculated using r decided by V as previously mentioned. Figure 8 shows the simulated bit error probability of the RPVD versus $\langle k_1\rangle$ for P_e=0.3 and 0.4, together with the bit

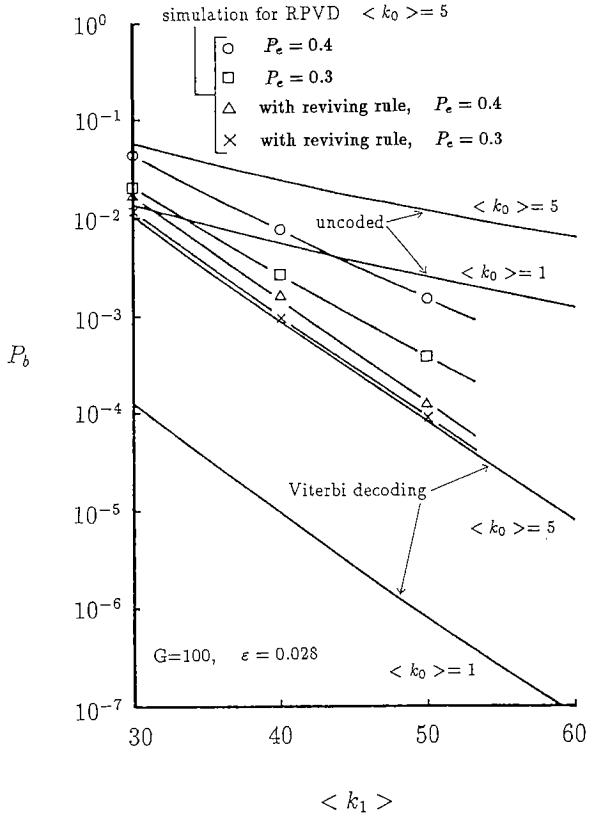

Fig. 8 Bit error probability in APD based receiver.

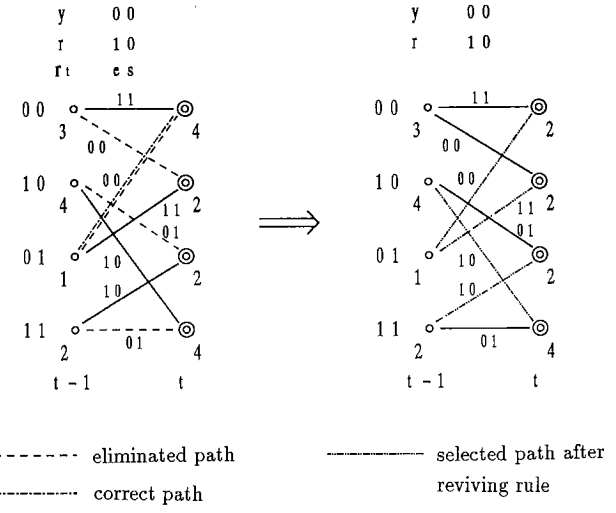

(a) Before employing reviving rule. (b) After employing reviving rule.

Fig. 9 An example applying reviving rule.

error probability for Viterbi decoding for $\langle k_0 \rangle = 1$ and 5. It is found that the bit error probability of the RPVD is more degraded compared with Viterbi decoding. It is because the branches of the correct path are eliminated when $r_t = e$ for $y = 0$.

To prevent this performance degradation, we employ the following reviving rule to revive the eliminated correct path. Let us assume the case that at a node level t some paths are eliminated and the minimum value of the path metrics (in the sense of Hamming distance) of all survival states increases than that of the previous level $t-1$. In such a case, we employ the following procedure. The eliminated paths are revived from the survival states at the node level $t-1$ and the metrics are recalculated at the node level t. We call this reviving rule.

Figure 9 shows a typical example employing the reviving rule. In Fig. 9(a), assume that the path metrics in the sense of Hamming distance on each state are 3, 4, 1 and 2, respectively, as denoted beside the states, and that $r_t = es$ and $r = 10$ for $y = 00$. The error occurs at the first symbol and the correct path is eliminated. The minimum metric of all states is 1 on state 01 at the node level $t-1$. At the next node level t, the minimum metric increases to 2, and then the reviving rule is employed. All the branches from the survival states at level $t-1$ are revived and the metric is recalculated and the survival paths are selected by ACS operations on the merged states as in Fig. 9(b). In this case, the correct path eliminated by branch elimination revives by the rule. On the practical channel with small error rate, such a case in which the minimum metric increases in the event of correct path elimination is predominant. Thus, the revival of the eliminated correct path can be expected in most cases. The simulated bit error probabilities using the reviving rule are also shown in Fig. 8 for $P_e = 0.4$ and 0.3. The results show that the degradation becomes negligible. This indicates that the eliminated correct paths are revived in most cases by applying this rule.

Let us consider the increment of the number of ACS operations due to the reviving rule. The reviving rule is employed when at least one channel error occurs. Since there are two received symbols by one node level for the code with rate 1/2, the probability P_{rv} employing the reviving rule is,

$$P_{rv} \leqq 2P_E. \tag{22}$$

The ACS operations are done at most 4 times whenever reviving rule is applied. Then, the increment of the number of ACS operations n_{rv} due to reviving rule is given by

$$n_{rv} \leqq 4P_{rv} \leqq 8P_E. \tag{23}$$

Thus, n_{rv} is practically negligible when P_E is very small. The results in this section show that the RPVD is effective even in noisy channel by employing the reviving rule, at least for the code in Fig. 3(a).

6. Conclusions

A fast Viterbi decoding technique, called RPVD, has been proposed for the optical channels. The RPVD reduces the number of ACS operations which occupies dominant part of Viterbi decoding, by eliminating the paths based on detected signal level on the asymmetric optical channels.

The properties of the RPVD are shown in noiseless photon counting channel. It is found that the number of ACS operations is reduced to 9% of conventional Viterbi decoding for $k = 3$ without degradation in the bit error probability. In the cases using APD-based receivers with dark current noise, the rule to decrease the performance degradation are presented. The results show that the RPVD can be applied to the noisy channels at a cost of negligible performance degradation.

Acknowledgment

This work was supported in part by the Saneyoshi scholarship foundation and Hoso-bunka foundation.

References

(1) Divsalar D., Gagliardi R. M. and Yuen J. H.: "PPM performance for Reed-Solomon decoding over an optical-RF relay link", IEEE Trans. Commun., **COM-32**, 3, pp. 302-305 (March 1984).
(2) Prati G. and Gagliardi R.: "Block encoding and decoding for the optical PPM channel", IEEE Trans. In. Theory, **IT-28**, 1, pp. 100-105 (Jan. 1982).
(3) Viterbi A. J.: "Convolutional codes and their performance in communication systems", IEEE Trans. Commun., **COM-19**, 5, pp. 751-772 (Oct. 1971).
(4) Oka I. and Endo I.: "Error performance for soft decision viterbi decoding over OOK optical space links", Trans. IECE Japan, **E69**, 9, pp. 932-939 (Sept. 1986).
(5) Shenoy A. and Johnson P.: "Serial implementation of Viterbi decoders", COMSAT Tech. Rev. **13**, 2, pp. 315-330 (1983).
(6) Charbit M. and Bendjaballah C.: "Probability of Error and Capacity of PPM photon counting channel", IEEE Trans. Commun., **COM-34**, pp. 600-605 (June 1986).
(7) Uyematsu T., Yamazaki K., Hirota O., Nakagawa M. and Sakaniwa K.: "Effect of Asymmetric Error Correcting Codes in Photon Communication Systems", Trans. IEICE, **E71**, 9 (Sept. 1988).
(8) Hirota O., Yamazaki K., Nakagawa M. and Ohya M.: "Properties of error correcting code using photon pulse", Trans. IECE Japan, **E69** , 9, pp. 917-919 (Sept. 1986).
(9) Yamazaki K., Hirota O., Nakagawa M., Uyematsu T. and Ohya M.: "Effect of error correcting code on photon communication with energy loss", Trans. IEICE **E70**, 8, pp. 689 (Aug. 1987).
(10) Abshire J. B.: "Performance of OOK and Low-order PPM Modulations in optical communications when using APD-based receivers", IEEE Trans. Commun., **COM-32**, 10, pp. 1140-1143 (Oct. 1984).

(11) McIntyre R. J.: "The distribution of gains in uniformly multipling avalanche photodiodes: Theory", IEEE Trans. Electron Devices, **ED-19**, pp. 703-712 (June 1972).
(12) Yashima H., Sasase I. and Mori S.: "A New Type of Viterbi Decoding with Path Reduction", Proc. Globecom '89, pp. 1714-1718 (Nov. 1989).

Hiroyuki Yashima was born in Mie, Japan in 1958. He received the B.E., M.E. and Ph. D. degrees in Electrical Engineering form Keio University in 1981, 1987 and 1990, respectively. Since 1990 he has been with the Department of Information and Computer Sciences at Saitama University, where he is currently an Associate Professor. His research interests include modulation and coding, optical communication systems and satellite communication systems. He received 1989 Society of Satellite Professionals International Scholarship Award. Dr. Yashima is a member of IEEE.

Jouji Suzuki was born in Ohita, Japan in 1932. He received the B. E. and Ph. D. degrees in Electrical Engineering from Tokyo Institute of Technology, in 1955 and 1964, respectively. From 1955 to 1989 he was with the Communications Research Laboratory (CRL, originally Radio Research Laboratories) of Ministory of Post and Telecommunications. During 1988-1989 he was the Director General of CRL. He is currently a Professor in the Department of Information and Computer Sciences at Saitama University, Japan. His research interests include speech communications and communication systems. Dr. Suzuki is a member of Acoustical Society of Japan, Acoustical Society of America and The Institute of Television Engineers of Japan.

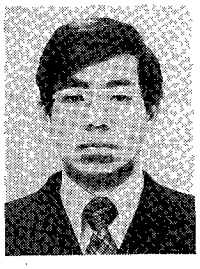

Iwao Sasase was born in Osaka in 1956. He received the B. E., M. E., and Ph. D. degrees in Electrical Engineering from Keio University, Yokohama, Japan in 1979, 1981 and 1984, respectively. From 1984 to 1986 he was a Post Doctoral Fellow and a Lecturer of Electrical Engineering at University of Ottawa, Canada. He is now an Assistant Professor of Electrical Engineering at Keio University, Japan. His research interests include modulation and coding, communication theory, and satellite communications. He received 1984 IEEE Communications Society Student Paper Award (Region 10). Dr. Sasase is a member of IEEE.

Shinsaku Mori was born in Kagoshima, Japan in 1932. He received the B. E., M. E., and Ph. D. degrees in Electrical Engineering from Keio University, Yokohama, Japan in 1957, 1959 and 1965, respectively. Since 1957, he has been engaged in research at Keio University, mainly on nonlinear circuit theory and communication engineering. He is now a Professor of Keio University. He is a member of Institute of Electrical Engineers of Japan and IEEE.